Superabsorbent polymer additives for repeated barrier restoration of damaged powder coatings under wet-dry cycles

A proof-of-concept

Saini, Vimal; von Tapavicza, Max; Eloo, Christina; Braesch, Katrin; Wack, Holger; Nellesen, Anke; Schmidt, Annette M.; García, Santiago J.

DOI
10.1016/j.porgcoat.2018.05.019

Publication date
2018

Document Version
Accepted author manuscript

Published in
Progress in Organic Coatings

Citation (APA)
Saini, V., von Tapavicza, M., Eloo, C., Braesch, K., Wack, H., Nellesen, A., Schmidt, A. M., & García, S. J. (2018). Superabsorbent polymer additives for repeated barrier restoration of damaged powder coatings under wet-dry cycles: A proof-of-concept. *Progress in Organic Coatings*, *122*, 129-137. https://doi.org/10.1016/j.porgcoat.2018.05.019

Prog.Org. Coat. 122 (2018) 129–137, https://doi.org/10.1016/j.porgcoat.2018.05.019

Superabsorbent polymer additives for repeated barrier restoration of damaged powder coatings under wet-dry cycles: a proof-of-concept

Vimal Saini[1,2,i], Max von Tapavicza[1,2], Christina Eloo[1] , Katrin Braesch[1], Holger Wack[1], Anke Nellesen[1], Annette M. Schmidt[1,2], Santiago J. García[3]

[1]Fraunhofer Institute for Environmental, Safety and Energy Technology UMSICHT, Osterfelder Str.3, 46047 Oberhausen, Germany

[2]University of Cologne, Chemistry Department, Luxemburger Str. 116, 50939 Köln, Germany

[3]Novel Aerospace Materials group, Faculty of Aerospace Engineering, Delft University of Technology, Kluyverweg 1, 2629 HS, Delft, The Netherlands

Corresponding author

Christina Eloo, Fraunhofer Institute for Environmental, Safety and Energy Technology UMSICHT, Osterfelder Str.3, 46047 Oberhausen, Germany

christina.eloo@umsicht.fraunhofer.de

Keywords

self-healing; powder coating; superabsorbent polymer; corrosion inhibition; electrochemical impedance spectroscopy

Abstract

Superabsorbent polymers (SAPs) are well known for their ability to absorb and hold high water amounts accompanied by a high volume expansion. In this work we show the benefits of this underlying property of SAPs to induce underwater crack closure with subsequent barrier restoration in damaged protective coatings. For the proof of concept, three layer epoxy-polyester (EP) powder coating systems were developed and applied on carbon steel. In these systems the middle EP layer (also called functional layer) contained crosslinked acrylamide/acrylic acid copolymer SAPs in different amounts ranging from 0 to 40 wt%. The capability of the SAPs to close damages and extend barrier and corrosion protection was evaluated by electrochemical impedance spectroscopy (EIS), NaCl aqueous solution immersion test and optical microscopy. It was found that coatings loaded with a 20 wt% SAP led to the best overall corrosion protection for the studied systems. In order to proof the potential use of this extrinsic healing concept for multiple healing events wet-dry cycles on scratched systems

[i] Present address: Elementis GmbH, Stolberger Straße 370, 50933 Köln

were performed and the corrosion performance was followed by EIS. Although not yet optimal, the results show the potential of the concept for multiple healing events under wet-dry conditions.

1 Introduction

Corrosion protection of metal structures using self-healing concepts has attracted significant attention in the last two decades. Such attention is based on the potential of the concept to restore local protection after damage by multiple strategies [1]. Two main self-healing generic strategies have been explored in anticorrosive coatings, namely intrinsic and extrinsic self-healing. Intrinsic self-healing implies that the healing capability is given by the matrix itself. In this concept temporary mobility of the matrix (e.g. polymeric coating) leads to damage restoration such as closure of scratches or recovery of adhesion [2]. Intrinsic healing can be obtained by using various types of reversible covalent and non-covalent chemistries such as ionomers [3], disulfide bridges [4], shape memory polymers [5] and Diels Alder moieties [6]. Extrinsic self-healing is obtained by secondary reactive phases added to the main matrix. The most common approaches use capsules containing reactive liquids [7] or inorganic nanoparticles loaded with corrosion inhibitors [8–12]. Despite the multiple strategies developed, clear benefits to extend the corrosion protection at damaged sites is still challenging due to some drawbacks. On the one hand most intrinsic healing principles require a localized energetic input which can limit future applications while extrinsic concepts using encapsulated liquids can only heal once and are technologically complex to upscale. Moreover most of the existing research has focused on solvent based coatings while the more environmentally friendly organic powder coatings [13–15] have attracted little to no attention. In this work we explore the potential of superabsorbent polymers to develop an extrinsic healing powder coating capable of repeated healing at the same damaged site with wet-dry cycles. Superabsorbent polymers (SAPs) have the ability to absorb liquids up to several thousand times of their own weight, keeping this water in the structure for long periods of time. Superabsorbent polymers are extensively used in baby diapers [16] and agriculture [17–20] but their use in self-healing coatings is limited to a handful of works. Yabuki et al. showed that a SAP could act as a self-healing agent in a vinyl-epoxy liquid coating [21] and some patents were filed showing the potential of SAPs for water blocking in optical cables [22]. SAPs have also been used to develop swellable thermoplastic/elastomer alloys [23], water-swellable rubbers [24] and self-healing concrete [25–27]. In all these concepts the underlying principle is the same: when there is damage, the SAP is exposed to the environment from where the SAP

absorbs humidity thereby expanding. The local expansion of the SAP leads to the blocking of the damage and protection of the underlying (metallic) structure by local barrier restoration.

In this work we show the potential use of SAPs as self-healing additives in powder coatings. To demonstrate the concept a three layered epoxy-polyester (EP) powder coating system was developed. Acrylamide/acrylic acid copolymer SAP was synthesized and incorporated in the coating system by blending it with the middle EP layer, this conforming the so called functional middle layer. Several coatings were prepared with different SAP concentrations in the middle layer ranging from 0 to 40 wt%. To evaluate the damage healing potential the coatings were manually scratched with a knife ensuring the underlying substrate was reached. The behavior of the coatings and their barrier restoration efficiencies were then evaluated by electrochemical impedance spectroscopy (EIS) and salt water immersion testing. The potential of the concept as an extrinsic healing strategy with multiple healing events at the same damaged site was evaluated by wet-dry cycles and EIS. The results are promising although more research is needed to improve the overall barrier restoration and healing repeatability at one same damaged site.

2 Materials and Experimental

2.1 Synthesis of SAP

Crosslinked acrylamide/acrylic acid superabsorbent copolymers (SAPs) were synthesized in the lab by radical polymerization. Acrylic acid (99 % purity; 0.02 % hydroquinone monomethyl ether as stabiliser) was supplied by Sigma–Aldrich Chemie GmbH. N,N'-methylene bisacrylamide (> 98 % purity), sodium hydroxide (> 98 % purity), ammonium persulfate (> 98 % purity) and sodium bisulfite (97–100 % purity) were supplied by Merck KGaA and used as received.

Acrylic acid (AA) and sodium acrylate (SA) were used as functional monomers and N,N-methylene bisacrylamide as a crosslinking monomer. The redox system ammonium persulfate and sodium bisulphate was used as the initiator. For the synthesis of SAP, 0.78 mol of AA was first dissolved in 16 mol of deionised water in an ice bath at 3°C. Subsequently, this mixture was neutralized with 0.58 mol of NaOH to achieve the required 75 mol% degree of neutralization of AA. After this, 0.04 mol of crosslinker was dissolved in the solution, which was then deaerated by bubbling with nitrogen for 10 min. Thereafter, the solution was cooled down to 10 $^{\circ}$C in an ice bath and stored for further 5 min. This monomer solution was then mixed with the initiator solution (0.01 mol of ammonium persulfate and 0.01 mol of sodium bisulphate dissolved in 10 ml of deionised water) and then transferred to a 500 ml glass bottle

at 60 °C to allow the polymerization reaction to proceed. The polymerization reaction was completed after 4 h. Thereafter, the hydrogel was taken out of the glass bottle and cut into small pieces. The hydrogel pieces were stored in deionised water at ambient temperature for four days for washing out of the unreacted components, at daily water exchange. The hydrogel was then dried in vacuum oven for 24 h at 70 °C and ground in a ball mill to obtain a powder. The resulting particles had a cubically broken geometry. The powder had an unimodal distribution with a d(0.1) of 15 µm, a d(0.5) of 42 µm and a d(0.9) of 76 µm.

2.2 Swelling degree of SAP

The tea bag method was used for the measurement of swelling degree of the synthesized SAP. About 0.2 g of SAP powder is sealed in a liquid-permeable tea bag and immersed in a bath of 5 wt% aqueous NaCl solution and kept at ambient temperature. The tea bag was then taken out at set intervals (1, 2, 5, 10, 15, 20, 30 and 60 min) and drained for one minute to remove the excess water before weighing. The equilibrated swelling (ES) was measured twice using the following equation

$$ES(g/g) = \frac{W_2 - W_1}{W_1} \quad \text{Eq. 1}$$

After weighing the swollen gels, the swelling degree (water absorption of SAP at a given moment) was calculated according to Eq. 1

2.3 Cyclic absorption-drying tests of the SAP

To identify any potential loss in the absorption potential of the SAPs up to four absorption-drying cycles were performed. During the absorption step the SAPs were immersed for one hour in 5 wt% aqueous NaCl solution until saturation was reached. The drying cycle consisted of exposing the saturated SAPs in an oven at 70 °C until full drying.

2.4 Coating systems preparation

Low carbon, cold rolled steel with a thickness of 0.8 mm and a size of 102 x 102 mm used as metal substrate was supplied by Q Lab Germany under the brand name R46, and used after degreasing. Epoxy-polyester powder coatings containing high performance epoxy and polyester resins were used as received from Axalta Coating Systems Germany GmbH with a particle size < 160 µm (brand name Aleasta EP). The EP powder coatings were deposited by electrostatic spraying onto the low carbon steel (at 60 kV potential difference) and cured in an oven at 170 °C for 10 min.

Based on preliminary tests it was decided to develop a three layer system in which the SAP particles are located in the middle (i.e. a functional coating as middle layer between a primer

and a topcoat). It should be noted that when the SAPs were added in the primer the coatings showed a clear adhesion loss and low resistance to water exposure, thereby highlighting the need for a primer below the SAP-containing layer. When the SAP-containing layer was directly exposed to water a fast and uncontrolled leaching of the SAP was observed with its consequent loss of healing potential. This highlighted the need for a barrier topcoat to force the SAP swelling and expansion to occur only at damaged sites. To form the three-layer coating systems first the base EP layer was applied and placed in an oven at 170 °C for 3 min to ensure sufficient melting and coverage. Then the functional middle EP layer containing the SAPs was applied using different EP/SAP powder mixtures (0 up to 40 wt% SAP) and placed in an oven at 170 °C for 3 min. Finally the last EP layer was deposited and the three-layer coating system cured in an oven at 170 °C for 10 min. A schematic of the process is depicted in Figure 1. The average coating thicknesses of all the samples was 245 µm (with a functional middle layer of approximately 104 µm thick and the base and top layers of 70 µm). To show the stability of the SAPs during the curing process at 170°C a dedicated thermogravimetric and differential scanning calorimetry analysis of the polyacrylate-based SAPs was performed. The results showed the particles are stable until up to 230 °C, well in agreement with previously published works with similar SAPs [28], and therefore stable during the coating curing process. Table 1 shows the different coating systems prepared and their nomenclature used along the manuscript.

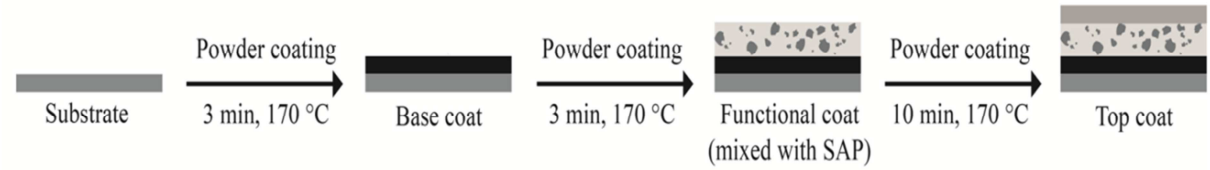

Figure 1:Three layer coating system production

Table 1: Coatings prepared with different SAP contents.

Sample	SAP content in the functional layer
SAP-0	No SAP
SAP-10	10 wt% SAP
SAP-20	20 wt% SAP
SAP-30	30 wt% SAP
SAP-40	40 wt% SAP

Figure 2 shows a cross-section of a three-layer coating system (SAP-40) in dry and swollen state. To allow for a smooth surface and a higher contrast the cross-sections of the coated panels were polished down to 320 grit (VSM, KK114F, P320). The micrographs were taken by a digital microscope. Although the three coating layers cannot be easily identified, the SAP particles are slightly visible before immersion and clearly distinguishable after immersion in DI for one hour (black areas within the middle layer). The optical images show that the swelling of the SAP particles does not significantly affect the overall coating system thickness.

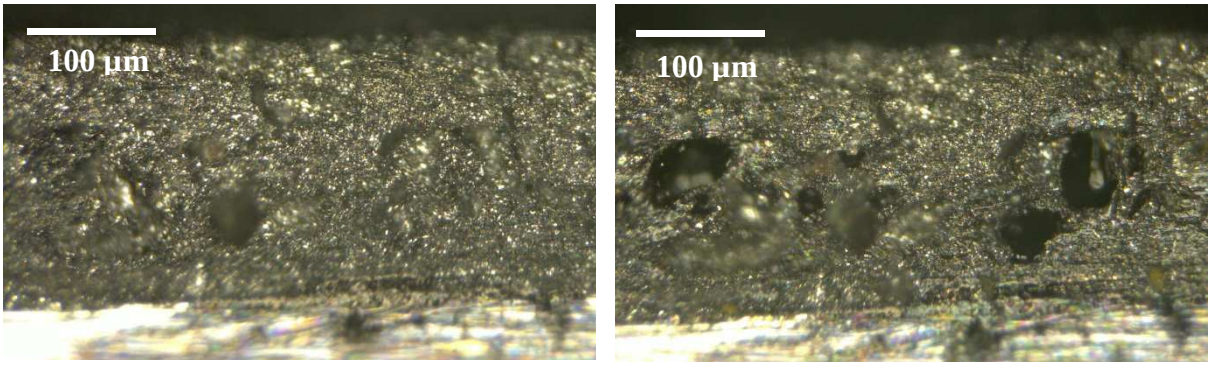

Figure 2: Micrographs of the cross-section of a three-layer SAP-40 coating system with SAPs in the middle layer in dry (left) and swollen state (right) after 1 h in de-ionized water. The SAP particles can be distinguished as dark areas in the middle of the coating.

2.5 Wet-dry cyclic immersion tests followed by EIS

Wet-dry cyclic tests were performed to analyze the potential of SAP particles to allow for multiple healing events at the same damage site. The barrier and corrosion protection performance was followed by electrochemical impedance spectroscopy (EIS) under immersion conditions. Repeats performed on the damaged coated systems as well as optical and salt fog spray confirmed the overall trends here reported, yet some differences in absolute measured values were found due to the impossibility to exactly reproduce the scratches.

For the EIS a potentiostat–galvanostat (autolab-PGSTAT30) and a frequency response analyzer (FRA) were used together with a faraday cage to avoid external interferences. A traditional EIS three electrode set-up was employed using Ag/AgCl as the reference electrode, platinum gauze as the counter electrode and the coated samples as the working electrode. All experiments were carried out at room temperature. The area of the working electrode was kept 16 cm^2 and 5 wt% NaCl aqueous solution was used as the electrolyte. The impedance measurements were carried out over a frequency range of 10^5 Hz to 10^{-2} Hz at 10 mV AC amplitude. Artificial defects of 200 µm width and 1 cm length were created in the coating systems with the help of a sharp knife before immersion. Before initiating the impedance test, the coating systems were allowed to stabilize at the open circuit potential for 10 min.

One wet-dry cycle consists of the following steps: the damaged sample is immersed in the electrolyte and EIS measurements performed instantly (t=0 h) and after one hour immersion (t=1 h), as this is the saturation time for SAPs as indicated in the swelling tests. After the EIS at 1 h immersion the electrolyte is decanted and the sample is dried in an oven at 60 °C for a period of one hour to ensure full drying in fast absorbing SAPs as the ones used in this work. After drying, the sample is immersed again in the electrolyte and a new EIS spectrum is recorded after one extra hour immersion. The wet-dry cycle was repeated three times. After the three cycles the samples were kept immersed in the electrolyte and a final EIS spectrum was recorded after 24 hours (t=24 h). A schematic diagram of this wet/dry cycles is shown in Figure 3.

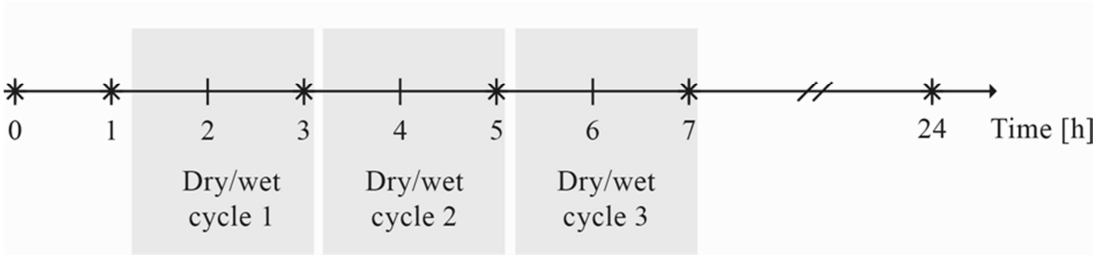

Figure 3: Schematic of the EIS cyclic test including the three dry/wet cycles during the full 24 h immersion test in 5 wt% NaCl. Stars represent the times at which an EIS spectrum was recorded.

2.6 Long term immersion tests

All coated samples with and without SAP (blank) were immersed in 5 wt% NaCl aqueous solutions for a period of 168 h to evaluate the corrosion behavior. Before exposure, the coated samples were manually scribed with the help of a sharp knife in T-shape according to the method described in DIN EN ISO 17872 norm to expose the underlying substrate to the corrosive environment. After the immersion tests, the samples were examined visually and with the help of an optical microscope. All experiments were replicated twice.

2.7 Optical microscopy

Optical microscopy was used to examine the distribution of SAP at the coating crack/scribe plane before and after the corrosion tests. Optical micrographs of the coatings with various amounts of SAP were also used to calculate the volume fraction of the SAP in the coatings which was further used for the calculation of theoretical maximal healing efficiency.

2.8 Adhesion tests

Adhesion tests were carried out before and after the immersion tests using a dedicated set up from Elcometer Instruments Ltd. The coated samples were tested for cross-hatch adhesion in agreement with the international standards: DIN EN ISO 2409, which involved scribing six

parallel cuts at 3 mm distance from each other through the coating. These cuts were then crossed afterwards by six perpendicular cuts. A soft brush was then applied to the coating for scraping off lifted coating. Adhesion loss was then followed using a magnifier lens.

3 Results and discussion

3.1 Characterization of SAP

The swelling degree of the synthesized SAPs with time in 5 wt% NaCl solution can be seen in Figure 4. The maximum swelling degree in this corrosive media is achieved already after 2 minutes immersion at room temperature. Based on this result it was decided to perform the EIS wet/dry cyclic tests in intervals of one hour wetting and 1 hour drying thereby ensuring that the SAPs reach their maximum expansion potential during each studied cycle.

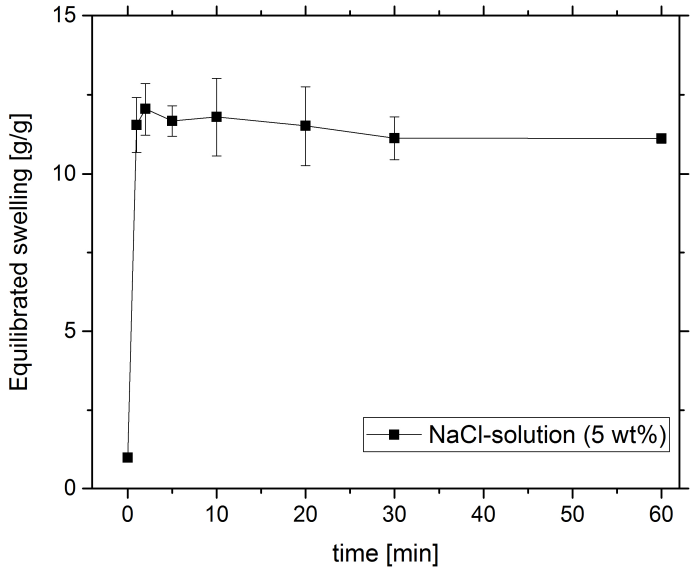

Figure 4: Swelling degree of SAP in 5 wt% NaCl solution. Measurements were done at 25 °C.

3.2 Self-healing mechanism by SAP containing coating layer

In the current study the SAP content was varied from 10 to 40 wt% in the functional layer of the coating (middle layer). Figure 5 shows a schematic design of the self-healing mechanism proposed under this concept. When the scratched coating comes in contact with water or the electrolyte used in this study (5 wt% NaCl in water), the SAP particles absorb water and swell to fill in and block the coating damage thereby hindering further electrolyte ingress.

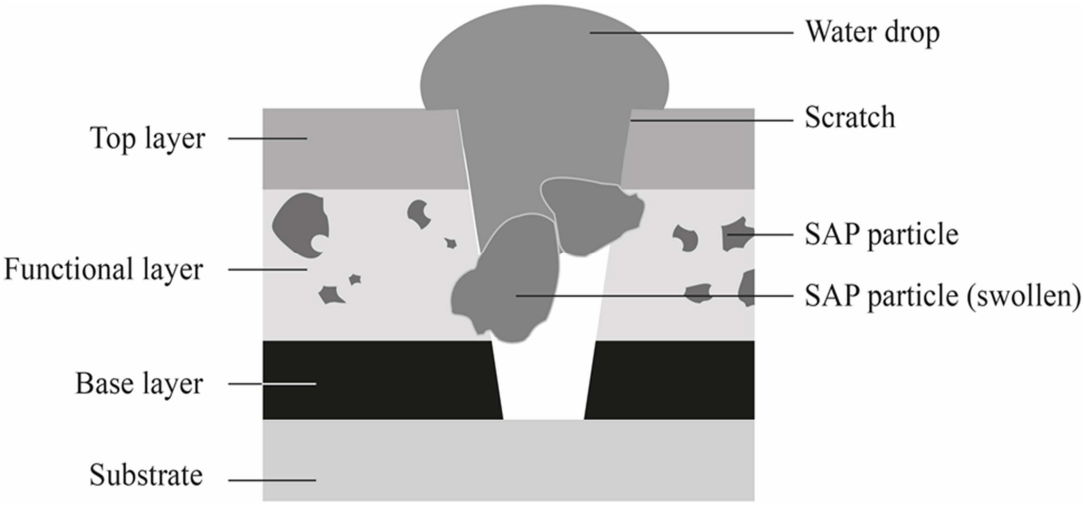

Figure 5: Idealized schematic representation of a three-layer coating system with SAP particles incorporated in the functional middle layer. The scheme shows the SAP particles swell when in contact with an electrolyte leading to the damage blocking by a high volume expansion.

The theoretical maximum scratch filling potential of the SAPs was calculated as the volume of the scratch divided by the swollen volume of the SAP particles available at the scratch plane. For the calculation several simplifications were taken: (i) the SAP particles are homogeneously distributed in the coating, show no particle size distribution and their diameter is assumed to be the same to their average particle size (i.e. 42 µm); (ii) when scratching, all the SAP particles and polymer lying in the scratch path will be removed from the scratch and only particles available at the wall sides will play a role in swelling; (iii) the scratch reaches the metal and is equally thick at its base as at the top. With all this the free volume of the scratch to be filled by the expanded SAP can be obtained by equation 2.

$$\text{Volume of the scratch } (V_{scratch}) = H_1 * L * W \approx 5 \cdot 10^8\ \mu m^3 \qquad \text{Eq. 2}$$

where: H_1 = total thickness of the coating system (245 µm); L= length of the scratch (10000 µm); W= width of the scratch (200 µm).

The volume that the swollen SAP particles can fill (V_{filled}) can be calculated according to equation 3 [29].

$$V_{filled} = \frac{\rho_{t} * \emptyset * H_2 * L * d * S_f}{\rho_p} \qquad \text{Eq. 3}$$

Where; $\rho_t = \frac{m_t}{V_t}$ (density of the coating); $\Phi = \frac{m_p}{m_t}$ (mass fraction of the SAP particle); $\rho_p = \frac{m_p}{V_p}$ (density of SAP particles); S_f= swelling degree of SAP particles (12 g/g in 5 wt% NaCl solution); L=length of the scratch (10000 µm); H_2= thickness of the functional layer (104 µm); d= average particle diameter of the SAP particles (42 µm).

Here: m_t= total mass of the coating, V_t= total volume of the coating; m_p= mass of the SAP particles, V_p = volume of the SAP particles. With this Eq. 3 can be rewritten as Eq. 4:

$$V_{filled}=\frac{V_p*H_{2*}L*d*S_f}{V_t}=f_v * H_2 * L * d * S_f \quad \text{Eq. 4}$$

Where $\frac{V_p}{V_t} = f_v$ (Volume fraction of the SAP particles)

The scratch filling efficiency **η** (%) by the SAP particles can be then calculated as

$$\boldsymbol{\eta(\%)} = \frac{V_{filled}}{V_{scratch}} = \frac{f_v*H_2*L*d*S_f}{H_1*L*W}=\frac{f_v*H_2*d*S_f}{H_1*W} \quad \text{Eq. 5}$$

It is seen from equation 5 that, for the same coating system dimensions, the scratch filling ratio is proportional to the diameter of the incorporated SAP particles (d), their volume fraction in the coating (f_v) and their swelling degree (S_f) but inversely related to the width of the scratch (W).

The actual volume fraction of the SAP in the coated samples was calculated by analyzing microscopy images of cross-sections of all the coating systems by image J software. The calculated volume fractions from the microscopy images are given in table 2.

Table 2: Mass fraction (Φ) and volume fraction (f_V) of the coatings with various amounts of SAP

Φ (%)	10	20	30	40
f_V (%)	5	13	17	21

By solving equations 4 and 5, Figure 6 is obtained. As it can be seen, the results can be fitted with a linear plot (Figure 6) revealing that when the volume fraction of SAP particles increases more volume of the scratch can be filled (higher scratch filling efficiency). At the same time the results also show that the SAP used in this study can only partially fill the performed scratches, reaching a maximum scratch volume filling near the 23 %.

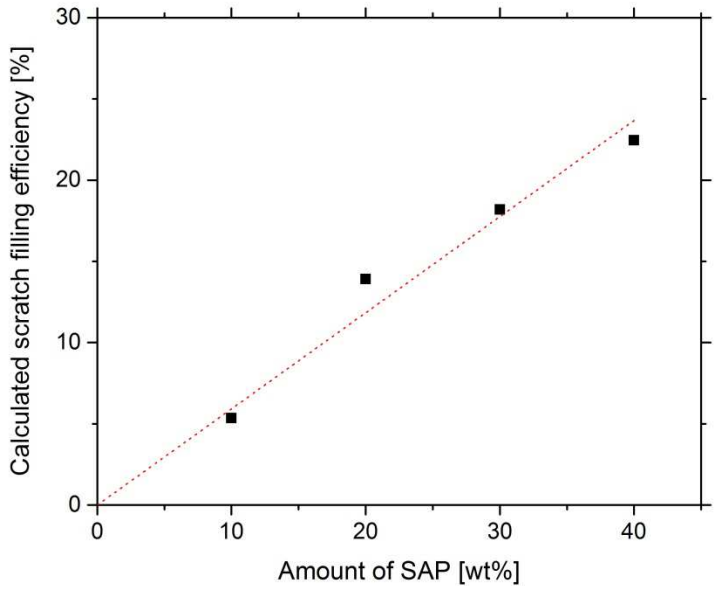

Figure 6: Calculated scratch filling efficiency **(η)** as function of the SAP vol% for a 200 µm wide scratch in 5 wt% NaCl solution. The dotted regression line confirms the expected linear result.

3.3 Effect of SAP content on barrier restoration of artificial scratches followed by EIS

Representative electrochemical impedance spectroscopy results of coated samples with and without SAP are shown in Figure 7. Results are displayed as Bode plots (i.e. impedance magnitude |Z| and phase angle vs. frequency). When comparing the impedance plots at short and long immersion times (t = 0 h, 1 h and 24 h) it was found that the low frequency impedance of coating systems with SAP content 0 up to 30 wt.% slightly increased in the first immersion hour. Such phenomenon at low frequencies can be attributed to opposite phenomena such as oxidation/passivation or barrier restoration action by the SAPs limiting surface redox processes. Differences become more clear when the overall impedance (whole frequency range) is observed. In this case it becomes clear that SAP-0 and SAP-10 show an overall sharp impedance drop in this first immersion hour, which is well in agreement with an absence of barrier restoration. Samples SAP-20 and SAP-30 show a more moderate impedance drop suggesting a moderate barrier restoration while SAP-40 shows an overall significant increase in the total impedance in the first hour of immersion thereby pointing at a positive effect of high SAP contents on the short term barrier restoration at a damage site.

At long immersion times (24h) differences between the coatings at different SAP contents are also remarkable. As expected, the coating system without SAP (SAP-0) shows a single time constant obvious in the phase angle at low frequencies along with very low total impedance in the entire frequency range indicating total barrier loss and active corrosion at the scribe [30]. The systems with SAP showed on the other hand two distinctive time constants (visible in phase and magnitude) and an increase of the impedance at the mid-frequency range when

compared to SAP-0 at different immersion times. While the time constant at lower frequencies can be attributed to activity at the metal surface, the time constant at mid-range frequencies can be attributed to (partial) barrier restoration at the scribe. This effect can only be justified by the expansion of the SAPs due to water absorption thereby limiting water ingress and active corrosion at the damaged site. Despite the similarities amongst the SAP containing systems it also becomes clear that SAP-20 behaves significantly better than the other systems. For this coating system the total impedance does not show any significant impedance drop in the studied frequency range during the evaluated immersion time (0-24h). Moreover the total impedance remains more stable and higher than that of the other systems. Such a result points at a high and stable barrier restoration in the case of SAP-20 coating system leading to lower activity at the metal substrate. These results suggest a possible optimal content of SAP in the functional coating layer near 20-30 wt.%.

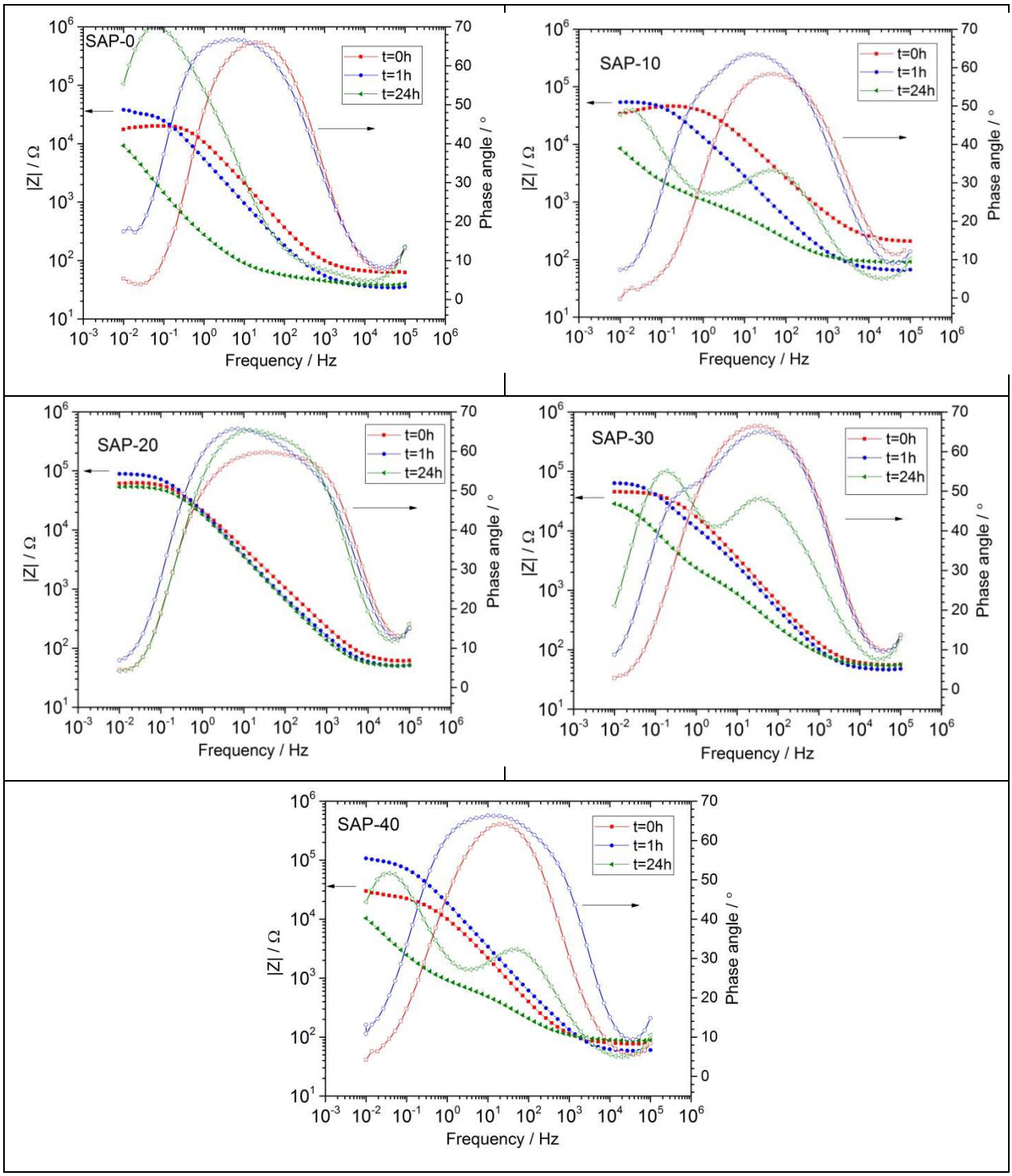

Figure 7: Bode plots of coated systems with different SAP contents (0 up to 40 wt% in the middle layer) with a 200 µm wide scratch exposed to 5 wt% NaCl solution.

Post mortem optical micrographs of all coatings after 24 hours immersion and electrochemical tests are shown in Figure 8. In these micrographs corrosion products can clearly be seen at the scratch of coating SAP-0 while no obvious corrosion products can be seen in the other coating systems containing different SAP contents. From the micrographs analysis it seems that low SAP contents (i.e. 10 wt%) do not lead to a clear filling of the scribe surface which is in

agreement with the low volume filling for low SAP contents and the EIS results. Higher SAP contents (20, 30 and 40 wt%) show a filled scratch surface in agreement with EIS even if based on theoretical calculations (Figure 6) it is possible to state that the SAP content was not sufficient to fully fill the scribes. Furthermore, it becomes apparent that higher SAP contents lead to blistering in regions close to the scribe which could justify the change in trend observed in EIS when SAP content was higher than 20 wt%. In the post-mortem analysis it was found that high SAP amounts (40 wt%) lead to an increase of the interface volume resulting in easy hand delamination of the whole coating. On the other hand, little to no corrosion was detected at the scribe of the coating systems SAP-20 and SAP-30 after removing the SAP layer at the scribe. In view of these results, a good correlation can be established with the EIS results showing significant barrier restoration in the coating systems with 20 and 30 wt% SAP content with an optimal SAP content in the range $10 < SAP_{optimal}$ (wt%) < 30. Interestingly, when compared to the maximum theoretical volume filling these results point at significant level of barrier restoration during the studied immersion times even when the damages cannot be completely filled by the expanded SAPs.

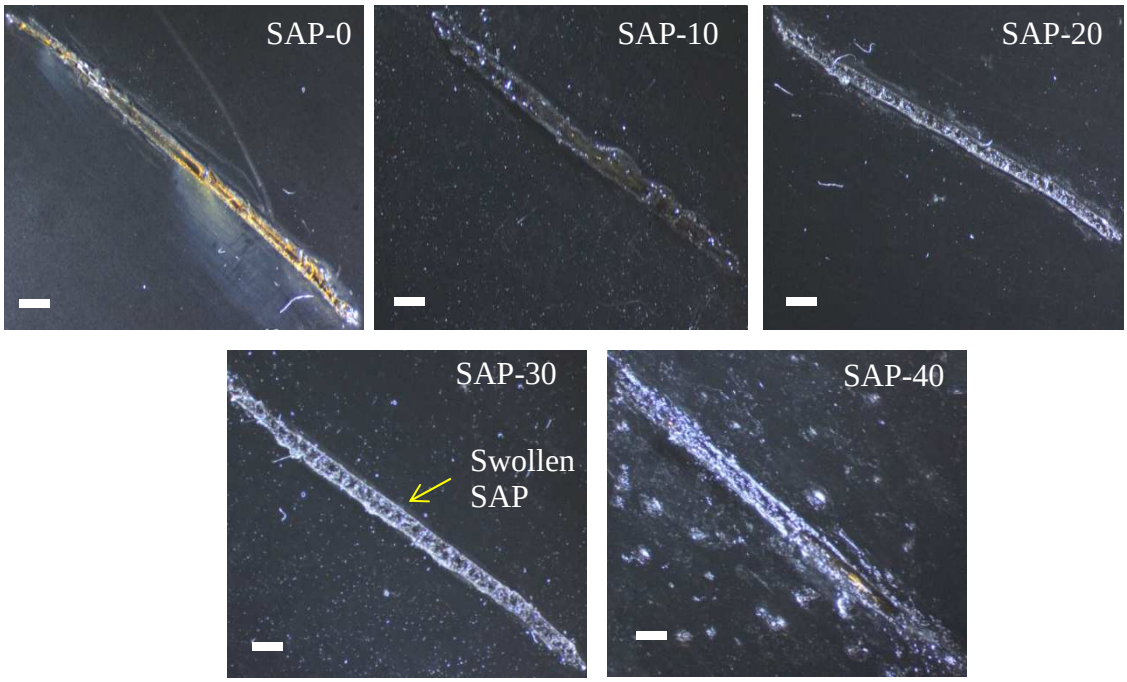

Figure 8: Optical micrographs of coating systems with different SAP contents (0 up to 40 wt% in the middle layer), after 24 h immersion and EIS tests in 5 wt% NaCl solution. Scale bars equal 0.5 mm.

3.4 Wet/dry cycles followed by EIS tests

Wet/dry tests were performed as represented in Figure 9 to evaluate the capability of the SAP to restore barrier at the same site multiple times during wet-dry cycles. The barrier restoration was evaluated by EIS during the wet cycle. Figure 9 a-e shows the Bode representation of the

EIS results after each wet/dry cycle. In this figure, it can be seen how the total impedance in the whole frequency range of the coating system without SAP (SAP-0) decreases continuously with the cycles highlighting the on-going degradation since first hour due to the expected lack of barrier restoration. Opposite to SAP-0, the coatings containing SAPs showed a varied effect with the wet-dry cycles. The impedance of SAP-10 dropped after the first wet-dry cycle while no significant variation in the subsequent cycles. A similar drop was detected in SAP-30 after the first dry cycle although in this case a second total impedance drop in the whole frequency range was observed after the second cycle to show no more significant changes after that. This points at a more robust system in the case of SAP-30 than SAP-10. Similar to SAP-30, SAP-40 showed two total impedance drops in the whole frequency range at cycles one and two. Nevertheless, contrary to SAP-30, impedance was recovered after the third cycle (impedance cycle 3 in Fig 9e). This last impedance increase in this sample could be due to passivation or oxides blocking the scratch or, less likely, to the higher amount of SAP overcoming the impedance loss due to further swelling. Moreover, as shown in 3.3, in this sample swelling led to blisters and delamination at longer immersion times (24 h) thereby affecting the overall EIS signal. A significantly better result compared to the other SAP-containing coatings was found for the coating system with SAP-20. In this case (Figure 9c), the impedance slightly drops during the first cycle but maintains a high impedance value in the whole frequency range during the cyclic test without significant variations. This clearly indicates a slow degradation of the SAP-20 coating system as well as the higher robustness of this coating against dry/wet cycles at the scribe.

A clearer trend is observed when the total impedance at low frequencies (0.01Hz) is plot against the wet/dry cycles as shown in Fig 9f. In this figure, the rapid decay of the total impedance with the wet/dry cycles in the high SAP containing coatings (SAP-30 and SAP-40) becomes evident. The total impedance of SAP-0 and SAP-10 decays more slowly although this could be related to the fact that the impedance is since t=1 h (cycle 0) already at values related to metal surface redox processes at the scribe (i.e. lack of barrier restoration at the scribe). SAP-20 on the other hand shows a relatively stable and higher impedance with the wet-dry cycles. Considering the total impedance value of the SAP-0 at one hour immersion, a minimum total impedance value above which low activity is observed can be drawn (dotted line Fig 9f). This simplified plot allows visualizing the superior behavior of SAP-20 and the drop in protection of the SAP-30 and SAP-40 in the second wet/dry cycles in a straight forward representation. Despite somewhat modest, the results here presented show for the first time the potential of an extrinsic healing concept based on swelling particles to offer multiple barrier

restoration events at damaged sites in coatings during wet-dry cycles. The results also highlight the presence of an optimal SAP content near 20 wt% (13 vol%) leading to sufficient gap filling yet without blistering and coating delamination caused by high water absorption in high SAP contents. Despite these results, more dedicated follow up works using the wet-dry EIS testing concept should be performed in order to evaluate the effect of the cycle-related stresses on the performance of healed scratches.

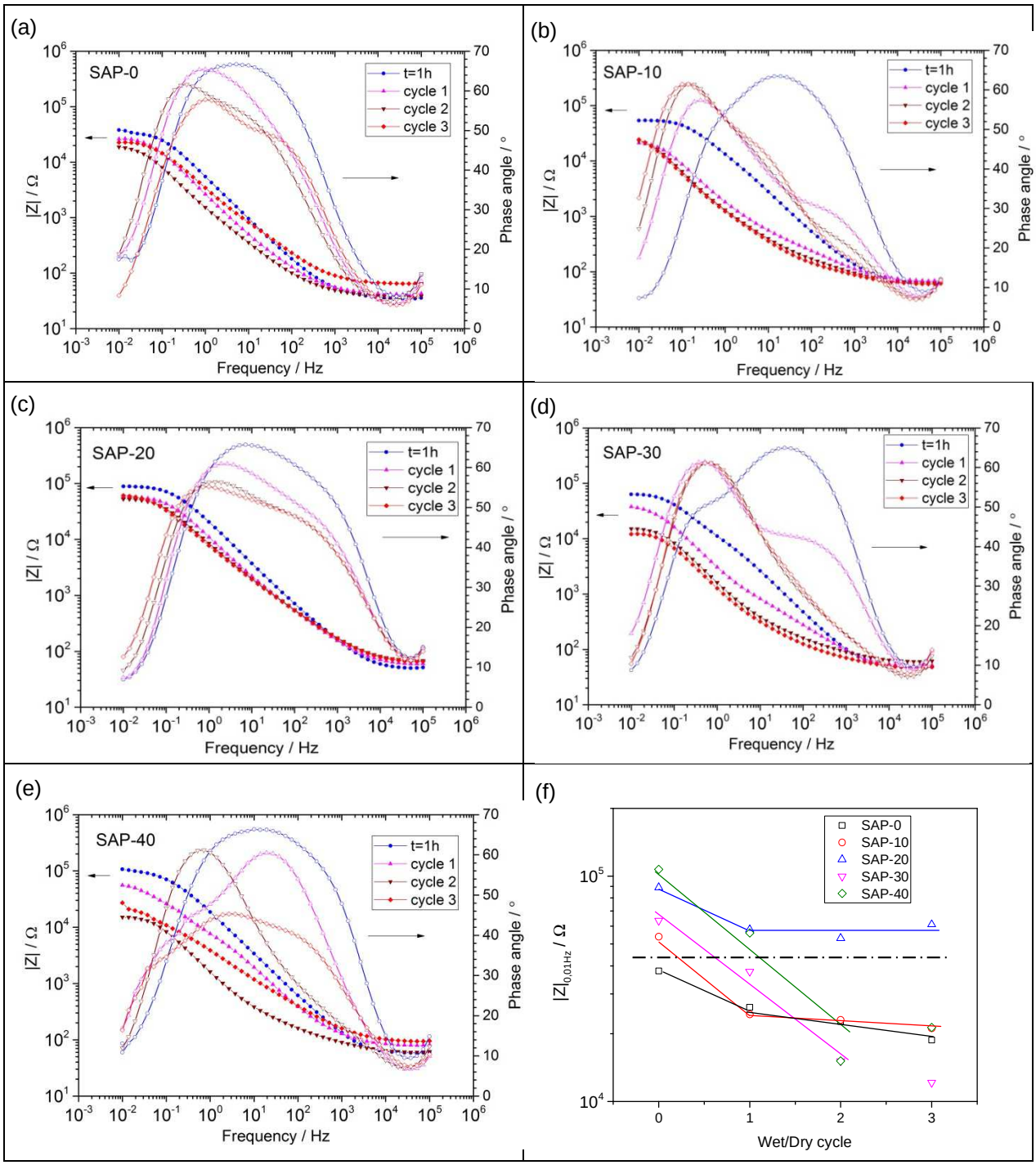

Figure 9: Wet/dry cycles of coated systems with different SAP contents (0 up to 40 wt% in the middle layer) with a 200 µm wide scratch exposed to 5 wt% NaCl solution (a—e). Figure 9f shows the total impedance at low frequencies (0.01Hz) for the five studied systems. Note: 0-cycles in Fig. 9f represent 1 h immersion in corrosive solution.

3.5 Long term immersion assessment by ISO 4628-8

For the long term corrosion tests, samples were immersed in 5 wt% NaCl solution for 168 hours at room temperature and evaluated according to ISO 4628-8. Before exposure, coatings were manually scratched with the help of a sharp knife to expose the underlying substrate to the corrosive environment. Figure 10 shows the optical microscopy images of the samples after

168 hours immersion. Table 3 shows the ranking of the coatings based on ISO 4628-8 image analysis. From the Table 3 and Figure 10 it can be concluded that the coating systems with SAP contents 20 wt% and 30 wt% showed the best corrosion performance in this test. However it should be noted that system SAP-30 in this case shows more blistering than SAP-20. These results further confirm those obtained by EIS that point at SAP-20 content as the best of the studied coating systems in terms of corrosion protection and overall coating behavior.

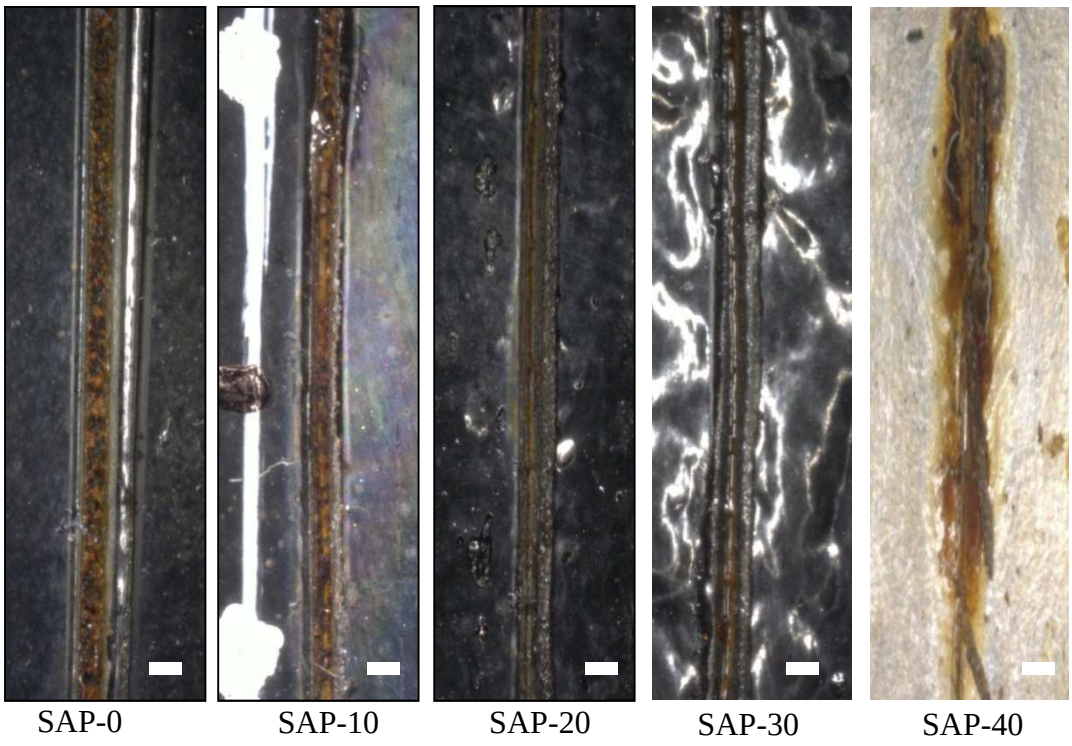

Figure 10: Coated panels after 168 h in 5 wt% NaCl solution. Scale length is 200 µm

3.6 Adhesion tests by DIN EN ISO 2409

Since coating's adhesion is a key parameter for the corrosion protection of metals together with barrier properties [30] dry and wet adhesion tests were performed. Table 3 shows the adhesion results evaluated as explained in the experimental section. As indicated in DIN EN ISO 2409 adhesion ratings of GT 0 represent no adhesion loss of the tested area, GT 1 represents 5 %, GT 2 represents 15 %, and GT 5 represents a complete delamination of the coating. As it can be seen all systems show good dry adhesion. Nevertheless, when exposed to the humid environment (5 wt% NaCl-water immersion tests for 168 h), the coating systems with high SAP contents show lower adhesion, being this remarkably detrimental in the case of SAP-40 and confirming the results obtained during the EIS tests where the best system is the SAP-20.

Table 3: Corrosion assessment by ISO 4628-8 and adhesion assessment by DIN EN ISO 2409.

Sample	Corrosion grade (ISO4628-8)	Adhesion before corrosion test	Adhesion after corrosion test
SAP-0	Grade 4 (Considerable)	GT0	GT1
SAP-10	Grade 4 (Considerable)	GT0	GT0
SAP-20	Grade 2 (Slight)	GT0	GT0
SAP-30	Grade 3 (Slight)	GT1	GT2
SAP-40	Grade 5 (Severe)	GT1	GT5

4 Conclusions

The potential use of superabsorbent polymers (SAPs) as healing agents in protective powder coatings has been presented and demonstrated by means of several methods yet considering the limitations of the experimental methodology used. The entire self-healing process was due to a barrier effect promoted by the local swelling of SAP particles at the damage site. The results shows that low SAP contents (<10 wt%) lead to low gap filling efficiency and therefore limited barrier restoration. On the other hand, high SAP contents (> 30 wt%) lead to higher gap filling efficiency (up to 25%) but low long term barrier restoration as well as blisters and delamination formed at long immersion times. It was found that, in the currently used non-optimized coating system, moderate SAP contents (near 20wt%; 13vol%) can lead for a short period of time to good and sustained barrier restoration combined with good dry and wet adhesion even if the scribe is not fully filled. Furthermore, the wet-dry cyclic EIS tests demonstrated the potential of the concept for repeated barrier restoration under such stress conditions without completely losing its protective capability for a number of cycles in the case of SAP contents around 20 wt%. Low and high SAP contents do not lead to a significant improvement in the overall coating performance or in the wet-dry cycle test suggesting an optimal SAP concentration might be located somewhere between 10 and 30 wt% in the studied system, seemingly at a content around 13 vol% (SAP-20). To the best of our knowledge this is the first proof-of-concept demonstrating the potential of SAPs to develop self-healing protective (powder) coatings. Due to the commercial availability and variety of SAPs and the ease of combination with corrosion inhibitors this type of self-healing principle is likely to be up-scaled and improved with relatively small amount of research in the topic. Nevertheless, in order to reach the full potential of the concept, more dedicated research around the coating system design and SAP selection should be performed. Special attention should be put on improving the elasticity of the coating layer containing the SAPs. It is expected that higher flexibility (as when more elastomeric layers are used) should lead to a better damage closure due to a local adaptation of

the coating to the SAP expansion and local elastic recovery helping gap closure. The durability in of healing concepts during wet-dry cycles should be regarded of outmost relevance when considering applications in which humidity varies in a cyclic manner during structure use such as in splash zones or transport containers.

Acknowledgments

The research leading to these results has received funding from the European Union Seventh Framework Programme (FP7/2007-2013) Marie Curie Action under grant agreement n° 290308 – SheMat as well as internal funding from Fraunhofer-Gesellschaft für angewandte Forschung e.V. (project number 826871).

References

[1] S.J. García, H.R. Fischer, S. van der Zwaag, A critical appraisal of the potential of self healing polymeric coatings, Progress in Organic Coatings 72 (3) (2011) 211–221.

[2] M. Abdolah Zadeh, S. van der Zwaag, S.J. Garcia, Adhesion and Long-Term Barrier Restoration of Intrinsic Self-Healing Hybrid Sol–Gel Coatings: ACS Appl. Mater. Interfaces 8 (2016) 4126–4136.

[3] R.K. Bose, N. Hohlbein, S.J. Garcia, A.M. Schmidt, S. van der Zwaag, Connecting supramolecular bond lifetime and network mobility for scratch healing in poly(butyl acrylate) ionomers containing sodium, zinc and cobalt, Physical chemistry chemical physics PCCP 17 (3) (2015) 1697–1704.

[4] M. Abdolah Zadeh, A.C. C. Esteves, S. van der Zwaag, S.J. Garcia, Healable dual organic-inorganic crosslinked sol-gel based polymers: Crosslinking density and tetrasulfide content effect, J. Polym. Sci. Part A: Polym. Chem. 52 (14) (2014) 1953–1961.

[5] A. Lutz, O. van den Berg, J. Wielant, I. de Graeve, H. Terryn, A Multiple-Action Self-Healing Coating, Front. Mater. 2 (2016) 1–12.

[6] M. Wouters, E. Craenmehr, K. Tempelaars, H. Fischer, N. Stroeks, J. van Zanten, Preparation and properties of a novel remendable coating concept, Progress in Organic Coatings 64 (2-3) (2009) 156–162.

[7] S.R. White, N.R. Sottos, P.H. Geubelle, J.S. Moore, M.R. Kessler, S.R. Sriram, E.N. Brown, S. Viswanathan, Autonomic healing of polymer composites, Nature 409 (6822) (2001) 794–797.

[8] M.L. Zheludkevich, S.K. Poznyak, L.M. Rodrigues, D. Raps, T. Hack, L.F. Dick, T. Nunes, M. Ferreira, Active protection coatings with layered double hydroxide nanocontainers of corrosion inhibitor, Corrosion Science 52 (2) (2010) 602–611.

[9] M.L. Zheludkevich, J. Tedim, M. Ferreira, "Smart" coatings for active corrosion protection based on multi-functional micro and nanocontainers, Electrochimica Acta 82 (2012) 314–323.

[10] M. Plawecka, D. Snihirova, B. Martins, K.Szczepanowicz, P. Warszynski, M.F. Montemor, Self healing ability of inhibitor-containing nanocapsules loaded in epoxy coatings applied on aluminium 5083 and galvanneal substrates, Electrochimica Acta 140 (2014) 282–293.

[11] G.L. Li, M. Schenderlein, Y. Men, H. Möhwald, D.G. Shchukin, Monodisperse Polymeric Core-Shell Nanocontainers for Organic Self-Healing Anticorrosion Coatings, Adv. Mater. Interfaces 1 (1) (2014) n/a.

[12] H. Wei, Y. Wang, J. Guo, N.Z. Shen, D. Jiang, X. Zhang, X. Yan, J. Zhu, Q. Wang, L. Shao, H. Lin, S. Wei, Z. Guo, Advanced micro/nanocapsules for self-healing smart anticorrosion coatings, J. Mater. Chem. A 3 (2) (2015) 469–480.

[13] E. Tang, G. Cheng, Q. Shang, X. Ma, A novel approach to the preparation of powder coating—Manufacture of polyacrylate powder coatings via one step minisuspension polymerization, Progress in Organic Coatings 57 (3) (2006) 282–287.

[14] A.G. Bailey, The science and technology of electrostatic powder spraying, transport and coating, Journal of Electrostatics 45 (2) (1998) 85–120.

[15] J. Fu, M. Krantz, H. Zhang, J. Zhu, H. Kuo, Y.M. Wang, K. Lis, Investigation of the recyclability of powder coatings, Powder Technology 211 (1) (2011) 38–45.

[16] K. Kosemund, H. Schlatter, J.L. Ochsenhirt, E.L. Krause, D.S. Marsman, G.N. Erasala, Safety evaluation of superabsorbent baby diapers, Regulatory toxicology and pharmacology RTP 53 (2) (2009) 81–89.

[17] F. Puoci, F. Iemma, U. G. Spizzirri, G. Cirillo, Polymer in Agriculture: a Review 3 (1) (2008) 299–314.

[18] M. Liu, R. Liang, F. Zhan, Z. Liu, A. Niu, Synthesis of a slow-release and superabsorbent nitrogen fertilizer and its properties, Polymers for Advanced Technologies 17 (2006) 430-438.

[19] J. Woodhouse, M.S. Johnson, Effect of superabsorbent polymers on survival and growth of crop seedlings, Agricultural Water Management 20 (1) (1991) 63–70.

[20] M.R. Guilherme, F.A. Aouada, A.R. Fajardo, A.F. Martins, A.T. Paulino, M.F. Davi, A.F. Rubira, E.C. Muniz, Superabsorbent hydrogels based on polysaccharides for application in agriculture as soil conditioner and nutrient carrier: A review, European Polymer Journal (2015).

[21] A. Yabuki, K. Okumura, Self-healing coatings using superabsorbent polymers for corrosion inhibition in carbon steel, Corrosion Science 59 (2012) 258–262.

[22] A.G. Bringuier, Siecor Operations, LLC Hickory. Indoor/outdoor optical cables - European Patent Office - EP 1014135 Al. December 17, 1999.

[23] H. Wack, D. Hintemann, H. Michael, N. Buschner, Preparation and properties of swellable thermoplastic elastomer alloys based on elastomeric powder, polypropylene, and superabsorbent polymer, J. Appl. Polym. Sci. 120 (3) (2011) 1290–1296.

[24] N. Dehbari, Y. Tang, Water swellable rubber composites: An update review from preparation to properties, J. Appl. Polym. Sci. 132 (46) (2015) 1–11.

[25] K. van Tittelboom, N. de Belie, Self-Healing in Cementitious Materials—A Review, Materials 6 (6) (2013) 2182–2217.

[26] D. Snoeck, K. van Tittelboom, S. Steuperaert, P. Dubruel, N. de Belie, Self-healing cementitious materials by the combination of microfibres and superabsorbent polymers, Journal of Intelligent Material Systems and Structures 25 (1) (2013) 13–24.

[27] D. Zhang, X.F. Song, T.S. He, Corrosion behaviour of reinforcing steel embedded in a concrete surface treated by in situ synthesised super-absorbent resin, Magazine of Concrete Research 65 (1) (2013) 63–70.

[28] S.-C. Liufu, H.-N. Xiao, Y.-P. Li, Thermal analysis and degradation mechanism of polyacrylate/ZnO nanocomposites, Polymer Degradation and Stability 87 (2005) 103-110.

[29] M. Huang, J. Yang, Salt spray and EIS studies on HDI microcapsule-based self-healing anticorrosive coatings, Progress in Organic Coatings 77 (1) (2014) 168–175.

[30] J. Li, L. Ecco, M. Fedel, V. Ermini, G. Delmas, J. Pan, In-situ AFM and EIS study of a solventborne alkyd coating with nanoclay for corrosion protection of carbon steel, Progress in Organic Coatings 87 (2015) 179–188.

[31] W.J. Soer, W. Ming, C.E. Koning, R.A. van Benthem, Towards anti-corrosion coatings from surfactant-free latexes based on maleic anhydride containing polymers, Progress in Organic Coatings 61 (2-4) (2008) 224–232.